



Cite this: *Dalton Trans.*, 2024, **53**, 17721

Antimony centre in three different roles: does donor strength or acceptor ability determine the bonding pattern?†

Richard Chlebík,^a Csilla Fekete,^b Roman Jambor,^b Aleš Růžička,^a Zoltán Benkő^{b,c} and Libor Dostál^a

A set of antimony(III) compounds containing a ligand (Ar) with a pendant guanidine function (where Ar = 2-[(Me₂N)₂C=N]C₆H₄) was prepared and characterized. This includes triorgano-**Ar₃Sb**, diorgano-**Ar₂SbCl** and monoorgano-**ArSbCl₂** compounds and they were characterized by ¹H and ¹³C NMR spectroscopy and by single-crystal X-ray diffraction analysis (sc-XRD). The coordination capability of **Ar₃Sb** and **Ar₂SbCl** was examined in the reactions with either *cis*-[PdCl₂(CH₃CN)₂] or PtCl₂ and complexes *cis*-[(κ^2 -Sb,N-**Ar₃Sb**)MCl₂] (M = Pd **1**, Pt **2**) and [(κ^3 -N,Sb,N-**Ar₂SbCl**)MCl₂] (M = Pd **3**, Pt **4**) were isolated, while their structures were determined by sc-XRD. Notably, the ligands **Ar₃Sb** and **Ar₂SbCl** exhibit different coordination modes – bidentate and tridentate, respectively – and the antimony exhibits three distinct bonding modes in complexes **1–4**, which were also subjected to theoretical studies.

Received 3rd October 2024,
Accepted 8th October 2024
DOI: 10.1039/d4dt02787f
rsc.li/dalton

Introduction

For a long time, triorganostibines have been considered heavier counterparts of ubiquitous phosphines regarding their coordination chemistry¹ and they usually behave as classical 2e L-type ligands. However, they also exhibit other interesting coordination properties, *e.g.* serving as bridging ligands, as demonstrated by Werner *et al.*² The family of Z-type ligands,³ that function as σ -acceptors for transition metals, has recently gained considerable attention. Although the first examples were reported as chemical curiosities in the 1970s as complexes with SO₂ or Ph₃Al,⁴ the main breakthrough started in the early 2000s.⁵ Examples of unsupported M \rightarrow Z interactions are also known in the literature,^{5a,6} but a majority of such interactions are mediated by pendant L donors that coordinate to the same central metal and simultaneously support the Z interaction.⁵ This concept often utilizes inherently Lewis

acidic group 13 elements,^{5,7} but systems based on other p-block elements⁸ including antimony⁹ have also emerged. The cornerstone in the field of antimony was laid by the Gabbaï group using the triphosphanylstibine Ar'₃Sb (Ar' = [2-(Ph₂P)C₆H₄]₃Sb) that after oxidation of the antimony atom revealed a Z-type Au \rightarrow Sb interaction (Fig. 1A).¹⁰ Since that time, various Au,¹¹ Ni,¹² Cu or Ag¹³ complexes profiting from this well-designed backbone have been reported. Ar'₃Sb or its congeners Ar'₂SbX (X = Ph or Cl) were also coordinated with PdCl₂¹⁴ and PtCl₂¹⁵ yielding Z-type complexes (*e.g.* Fig. 1B), while a new Sb–Cl bond formed due to the coordination non-innocent behaviour of the ligands. However, all the examples mentioned above rely on the utilization of phosphines as necessary supporting donors. A system bearing guanidine pendant functions, *i.e.* **Ar₃Sb** (Ar = 2-[(Me₂N)₂C=N]C₆H₄) has only recently been introduced into Cu or Ag chemistry, including remarkable coordination of the single Sb donor toward the M₃X₃ (M = Cu or Ag; X = halide) fragment using its 5s lone pair.¹⁶ As one may expect different donor properties of the

^aDepartment of General and Inorganic Chemistry, University of Pardubice, Studentská 573, CZ 532 10 Pardubice, Czech Republic. E-mail: libor.dostal@upce.cz

^bDepartment of Inorganic and Analytical Chemistry, Budapest University of Technology and Economics, Műegyetem rkp 3, H-1111 Budapest, Hungary. E-mail: benko.zoltan@vbk.bme.hu

^cHUN-REN-BME Computation Driven Chemistry Research Group, Műegyetem rkp 3, H-1111 Budapest, Hungary

† Electronic supplementary information (ESI) available: All experimental data including NMR spectra and theoretical studies. CCDC 2313661 (**Ar₃SbCl**); 2313662 (**Ar₂SbCl**); 2313664 (**Ar₃Sb**); 2313665 (**1**); 2313666 (**2**); 2313660 (**3**); 2313659 (**4**). For ESI and crystallographic data in CIF or other electronic format see DOI: <https://doi.org/10.1039/d4dt02787f>

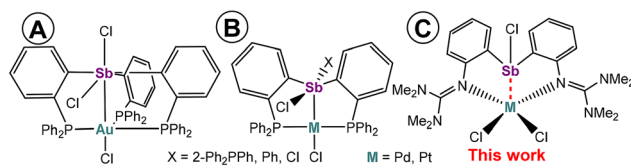


Fig. 1 Examples of Z-type ligands based on the antimony σ -acceptor (A and B) and complexes from the current study (C).



pendant imino-group in Ar compared to a phosphino-one in Ar', we herein examine this point and report on the coordination behaviour of **Ar₃Sb** and **Ar₂SbCl** in Pd(II) and Pt(II) complexes. Antimony is found in three distinct bonding modes, including a Z-interaction in five-coordinate complexes (Fig. 1C). However, no coordination non-innocence was observed for these ligands, thus differing from the phosphorus-based systems known so far (*cf.* Fig. 1B).

Results and discussion

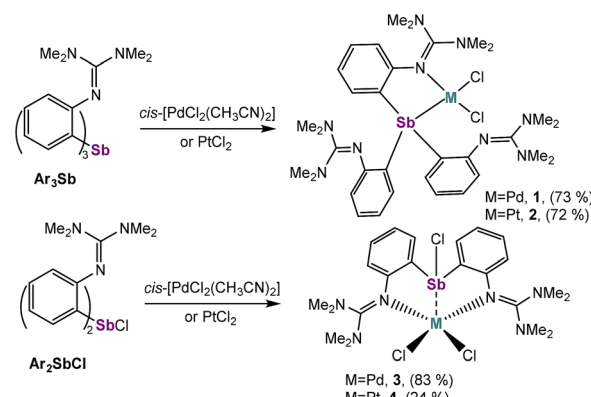
Treatment of the lithium precursor ArLi¹⁷ with SbCl₃ in an appropriate stoichiometric ratio furnished a set of organoantimony compounds **Ar₃Sb** (67%), **Ar₂SbCl** (58%) and **Ar₂SbCl₂** (49%). The ¹H and ¹³C NMR spectra revealed one set of signals for all the studied compounds (see the ESI†), including the typical signal for the guanidine N₃C carbon atom (δ (¹³C) in the range 157.6–159.2 ppm). This fact proves the magnetic equivalence of all Ar groups, indicating that the fluxional behavior of these compounds is rapid on the NMR time scale. Molecular structures were also determined by sc-XRD analysis (Fig. 2).

In the case of **Ar₃Sb**, the central atom adopts the expected trigonal pyramidal geometry. All the Sb–N distances (in the range 2.983(2)–3.059(2) Å) are similar to each other and are far longer than expected for a Sb–N covalent bond ($\Sigma_{\text{cov}}(\text{Sb}, \text{N}) = 2.11$ Å),¹⁸ thereby ruling out any significant intramolecular N → Sb interaction. In contrast, there is an obvious difference between the Sb1–N1/2 distances in **Ar₂SbCl**, *i.e.* 2.5440(17) vs. 3.0906(18) Å. These values are comparable to those of the related compound [2-(Me₂N)C₆H₄]Sb(Mes)Cl (2.619(3) Å),¹⁹ Finally, the Sb1–N1 distance of 2.4382(15) Å is the shortest in this series being consistent with the highest Lewis acidity of the central atom, but slightly longer than in, *e.g.*, [2-(Me₂NCH₂)C₆H₄]SbCl₂ (2.407(5) Å)²⁰ and [2-(DippN=CH)C₆H₄]SbCl₂ (2.416(2) Å).²¹ The enhanced Lewis acidity of the anti-

mony atom also leads to the formation of intermolecular Sb(1)–Cl(1)…Sb(1a) contacts (3.225 Å; *cf.* $\Sigma_{\text{cov}}(\text{Sb}, \text{Cl}) = 2.39$ Å).¹⁸

Their coordination toward either *cis*-[PdCl₂(CH₃CN)₂] or PtCl₂ was examined. Unfortunately, no stable complexes could be isolated from the respective reactions with **Ar₃SbCl₂**. Nevertheless, **Ar₃Sb** and **Ar₂SbCl** provided the compounds *cis*-[κ^2 -Sb,N-**Ar₃Sb**]MCl₂ (M = Pd 1, Pt 2) and [κ^3 -N,Sb,N-**Ar₂SbCl**]MCl₂ (M = Pd 3, Pt 4, Scheme 1), respectively.

Ar₃Sb behaves as an Sb,N-chelate in 1 and 2 containing tetracoordinated Pd and Pt centers in a square planar coordination environment (Fig. 3). To our knowledge, these complexes represent rare structurally characterized examples containing five-membered C₂SbNM metallacycles (M = Pd or Pt) as only a few related six-membered metallacycles have been reported: *i.e.* *cis*-[κ^2 -Sb,N-(2-(Me₂NCH₂)C₆H₄SbMes₂)PdCl₂],²² *cis*-[κ^2 -Sb,N-(2,6-(Me₂NCH₂)₂C₆H₃SbPh₂)PtCl₂],²³ *cis*-[κ^2 -Sb,N-(2-(Me₂NCH₂)C₆H₃)₃SbPtCl₂]²⁴ and *cis*-[κ^2 -Sb,N-(2-(Me₂NCH₂)Fc)₃SbPtCl₂].²⁵ The Sb1–Pd/Pt bond lengths of 2.4573(7)/2.4661(7) Å in 1/2 are a little shorter than those found in the abovementioned six-membered cycles (*cf.* Sb–Pd 2.4831(5) and Sb–Pt 2.4935(5)–2.5162(4) Å) and the same applies to the N1–Pd/Pt bonds of 2.082(3)/2.072(5) Å (*cf.* literature data 2.096(5)–2.133(4) Å).^{22–25}



Scheme 1 Synthesis of the investigated complexes.

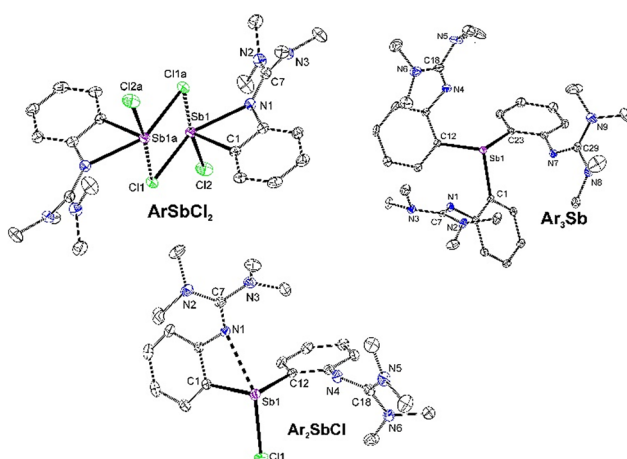


Fig. 2 Molecular structure of starting antimony compounds showing 30% probability ellipsoids and the crystallographic numbering scheme. Hydrogen atoms are omitted for clarity.

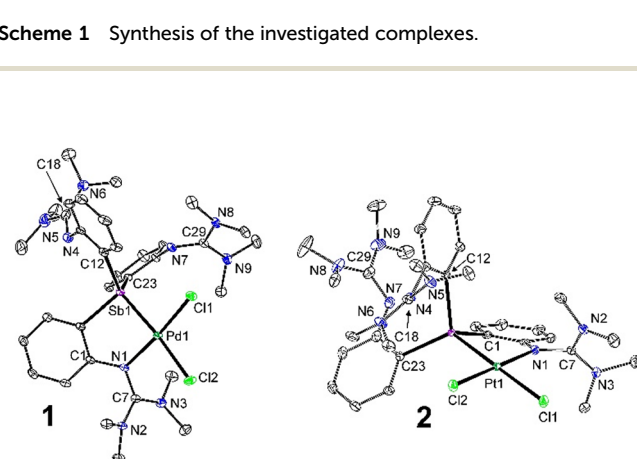


Fig. 3 Molecular structures of 1 and 2 showing 30% probability ellipsoids and the crystallographic numbering scheme. Hydrogen atoms are omitted for clarity.



The M–Cl bond located *trans* to the antimony is elongated to 2.4004(12) \AA in **1** and 2.3863(14) \AA in **2**. In line with the solid-state structures, the ^1H and ^{13}C NMR spectra of **1** and **2** revealed two sets of signals for the aryl ligands in a 1 : 2 integral ratio, indicating that only one of the guanidines forms a chelate with the metal. The methyl groups within this set of signals are magnetically non-equivalent ($\delta(^{13}\text{C}) = 40.4/41.7$ and 40.1/42.0 ppm, for **1** and **2**, respectively) suggesting hindered rotation around the phenyl–N bond due to the closure of this metallacycle. The formation of the chelate is also reflected in a pronounced down-field shift of one of the guanidine carbons N_3C 159.4/168.9 and 159.9/169.6 ppm in **1** and **2**, respectively, and this is also consistent with the value found in the non-coordinated parent Ar_2SbCl (158.9 ppm). Although both compounds were shown to be unstable at elevated temperatures by high-temperature ^1H NMR experiments (Fig. S17 and S18 \dagger), the ^1H , ^1H -EXSY experiment (with a mixing time of 1 s) in the case of palladium complex **1** clearly showed chemical exchange between all accessible guanidine donors in solution (Fig. S10 \dagger), proving its dynamic behavior. In contrast, similar experiments with **2** (with a mixing time of up to 3 s) revealed chemical exchange only in the region of the methyl groups of the coordinated guanidine function, while solely NOESY cross-peaks were obtained in the aromatic region of the spectra (Fig. S14–S16 \dagger). This suggests that the metallacycle in complex **2** is more rigid in solution.

In marked contrast to the conventional coordination mode in **1** and **2**, Ar_2SbCl in **3** and **4** behaves as an $\text{N}_2\text{Sb}_2\text{N}$ -pincer ligand (Scheme 1 and Fig. 4) pointing to a Z-type coordination of the antimony atom (*vide infra*). The central metals are coordinated by two chlorine and two nitrogen atoms in a *cis* fashion. The M–N (2.055(3) and 2.060(3) \AA for **3**; 2.049(5) and 2.049(7) \AA for **4**) and M–Cl bond lengths (2.3004(10) and 2.3138(10) \AA for **3**; 2.3085(18) and 2.319(2) \AA for **4**) are in the expected range for single bonds (*cf.* $\Sigma_{\text{cov}}(\text{Pd}/\text{Pt}, \text{N}) = 1.91/1.94 \text{\AA}$; $\Sigma_{\text{cov}}(\text{Pd}/\text{Pt}, \text{Cl}) = 2.19/2.22 \text{\AA}$).¹⁸ Importantly, the coordination number of the metals is increased to five by the coordination of the antimony atom, giving rise to a distorted square-pyramidal geometry for the Pt and Pd atoms. The atoms-in-molecules (AIM) study (see the ESI \dagger) also located five bond

critical points around the Pd/Pt centers ($\omega\text{B97X-D/def2-TZVP}$ level). This observation contrasts with the coordination non-innocent behaviour of the related systems containing pendant P-donors, where the coordination is accompanied by the formation of a new Sb–Cl bond, thereby preserving the square planar environment at the metal centers (Fig. 1B).^{14b, 15b, i} The bond lengths Pd–Sb 2.8829(5) \AA in **3** and Pt–Sb 2.8163(6) in **4** are elongated compared to those in **1/2** and with the closest counterparts from Fig. 1B (R = Cl), *cf.* Sb–Pd 2.4230(3)^{14b} and Sb–Pt 2.4407(5) \AA .^{15b} Nevertheless both values are still close to the respective $\Sigma_{\text{cov}}(\text{Pd}/\text{Pt}, \text{Sb}) = 2.60/2.63 \text{\AA}$ ¹⁸ indicating significant bonding interactions (*vide infra*). The coordination sphere of the antimony atom in **3** and **4** is completed by a chlorine atom (Sb–Cl 2.4605(12)/2.515(2) \AA for **3/4**) that is coordinated *trans* to the metal (Cl–Sb–M 171.35(3)/170.91(5) $^\circ$ for **3/4**) and is best described as having a see-saw geometry bearing a stereochemically active lone pair. Although complex **4** after isolation remains insoluble, the solubility of **3** was at an acceptable level that allowed recording of ^1H and ^{13}C NMR spectra, which revealed two sets of signals for both ligands in a mutual 1 : 1 integral ratio. The chemical shifts of both N_3C guanidine carbons at 165.9/169.9 are consistent with coordination toward the palladium atom, when compared with the values found in **1** and **2** (*vide supra*).

To explore the bonding situations in the experimentally obtained complexes, quantum chemical calculations were performed using various DFT functionals ($\omega\text{B97X-D}$, BP86, BP86-D3, B3LYP-D3, and M06-2X) in combination with the def2-TZVP basis set and the more accurate LNO-CCSD(T)/aug-cc-pVTZ level. Based on comparing the computed geometrical parameters with those obtained from sc-XRD experiments, the $\omega\text{B97X-D}$ (and BP86-D3) functional shows the best performance and, in the following, we only discuss the findings obtained at the $\omega\text{B97X-D/def2-TZVP}$ level. To scrutinize the nature of possible metal–antimony interactions that may stabilize these complexes, we performed NBO (Natural Bonding Orbital) calculations. In the case of complexes **1** and **2**, two important stabilizing donor–acceptor interactions were found: one from the N atom and another from the Sb center into the $\sigma^*(\text{M–Cl})$ antibonding orbital (Fig. 5A). In contrast, for the Pd–Sb interaction in complex **3**, the NBO analysis identifies two different types of interactions that are similar to those in a previous Au complex reported by the Gabbaï group:^{11a} (i) a donation from the d-orbital at the palladium center into the σ^* antibonding orbital of the Sb–Cl bond, $\text{lp}(\text{Pd}) \rightarrow \sigma^*(\text{Sb–Cl})$ (Fig. 5B), with a stabilization energy of only $E^{(2)} = 10.6 \text{ kcal}$

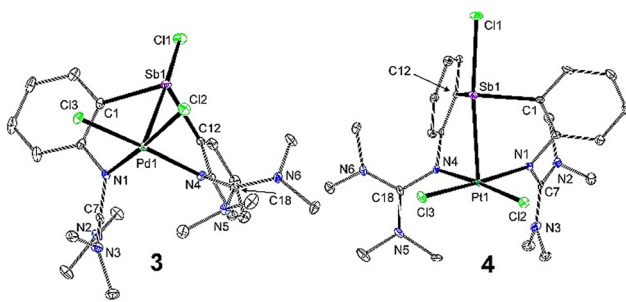


Fig. 4 Molecular structure of **3** and **4** showing 30% probability ellipsoids and the crystallographic numbering scheme. Hydrogen atoms are omitted for clarity.

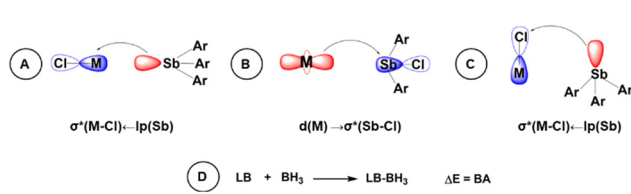


Fig. 5 Various M–Sb bonding interactions obtained in **1–4** (A–C) and the definition of borane affinity used in the study (D).

mol⁻¹ (according to the second order perturbation theory in the Fock matrix); and (ii) additional interactions arising from a donation of the s-type Sb lone pair toward the $\sigma^*(\text{Pd}-\text{Cl})$ orbitals with a summarized stabilization energy of 8.1 kcal mol⁻¹ (Fig. 5C). Although complex **4** shows similar characteristics, (i) the donation from the d-type Pt “lone pair” into the $\sigma^*(\text{Sb}-\text{Cl})$ orbital exhibits a significantly larger $E^{(2)}$ of 25.7 kcal mol⁻¹ (compared to **3**), while (ii) the two $\text{lp}(\text{Sb}) \rightarrow \sigma^*(\text{Pt}-\text{Cl})$ donations have a lower cumulative stabilization energy of 7.5 kcal mol⁻¹. The deletion procedures on the Fock matrix elements (for the interactions between the Sb–metal and Sb–Cl) in both **3** and **4** also delivered similar results for the $E^{(2)}$ values.

These donor–acceptor interactions also affect the geometrical parameters. On one hand, the backdonation from the M center into the $\sigma^*(\text{Sb}-\text{Cl})$ antibonding orbital is manifested in the slight elongation of the Sb–Cl bond in both complexes (2.461/2.515 Å, for **3/4**) compared to the free ligand **Ar₂SbCl** (2.442 Å). On the other hand, we focused on gaining evidence for the presence of the stabilizing interaction from the Sb lone pair toward the M center. Therefore, the lone pair of Sb was blocked by a BH₃ molecule in complexes **3** and **4** to hamper the $\text{lp}(\text{Sb}) \rightarrow \sigma^*(\text{M}-\text{Cl})$ donation. As a result, the Sb–M bond distance lengthens significantly upon the BH₃ addition from 2.88 to 3.17 Å for complex **3**, and a smaller but still notable change from 2.81 to 3.04 Å is observed for complex **4**. These Sb–M bond elongations are consistent with the lack of stabilizing interaction from the Sb center toward the metal in the borane adducts.

Finally, we aimed to identify the reasons why the **Ar₃Sb** and **Ar₂SbCl** ligands prefer different kinds of coordination modes. A simple and straightforward explanation seems to be the higher Lewis acidity of the **Ar₂SbCl** ligand compared to that of the **Ar₃Sb** counterpart. However, the backdonation in the Pd complex **3** offers stabilization similar to that of the Sb \rightarrow Pd donation, and this does not justify the formation of a pentacoordinate Pd center. To clarify this situation, we studied the borane affinities (BA, Fig. 5D) of the ligands at both Sb and N centers defined as the complexation energy of the donor center (LB, Lewis base) utilizing BH₃ as the Lewis acid (which cannot offer backdonation). The BA of the Sb center in the **Ar₃Sb** ligand is much lower (−32.4 kcal mol⁻¹) than that in **Ar₂SbCl** (−14.4 kcal mol⁻¹), highlighting that the Sb in the **Ar₂SbCl** ligand is a weaker donor than that in **Ar₃Sb**. Interestingly, the BA of the nitrogen in a guanidine arm (−24.4 kcal mol⁻¹) has a value intermediate between the BAs of the two types of Sb centers. Comparing the BAs of the various centers in these ligands reveals that the best stabilization using the triaryl ligand **Ar₃Sb** can be achieved *via* bidentate coordination utilizing the Sb and N donors.

In contrast to the **Ar₃Sb** ligand, the Sb center of the **Ar₂SbCl** ligand cannot compete with another N donor due to its highest (least negative) BA among the studied ones, and thus coordination is established by two imino-N centers rather than by an Sb and N donor. Altogether, the reason for the coordination fashion observed for complexes **3** and **4** is the lower donor strength of the Sb center compared to that of an imino-group rather than its higher Lewis acidity.

Conclusions

In conclusion, herein, we presented the synthesis and characterization of triaryl and monochloro-diaryl stibine Pd(II) and Pt(II) complexes displaying remarkably different molecular structures. Importantly, the Sb center in these complexes exhibits three different kinds of bonding: in the triaryl ligand **Ar₃Sb**, it behaves as a conventional Lewis base, and its donor ability clearly exceeds that of an imino-N center. The situation with the ligand **Ar₂SbCl** is more complicated: in its Pd complex, two different kinds of weak donor–acceptor interactions are established between the Pd and Sb centers. In one of these interactions, the Sb center acts as a donor (and the acceptor is the $\sigma^*(\text{Pd}-\text{Cl})$ orbital), while in the other, backbonding interaction, the $\sigma^*(\text{Sb}-\text{Cl})$ orbital accepts the electron density from the filled d-orbital at Pd. Moreover, the magnitudes of these stabilization effects (in reverse directions) are quite similar. In contrast to the Pd complex, in the Pt complex of **Ar₂SbCl** the donation of the Sb lone pair is clearly suppressed by backdonation, showing that the Pt center is a better donor than Pd. Our results indicate that the primary driving force for these different coordination modes lies in the lower donor strength of the Sb center in **Ar₂SbCl** than its higher Lewis acidity compared to **Ar₃Sb**. It is also noteworthy that the utilization of this guanidine-based ligand may allow for different coordination modes in comparison with well-established Gabbaï systems. We note that during proceeding of this paper, two related works dealing with nitrogen donors containing antimony ligands in Z-type coordination appeared in the literature.^{26,27}

Experimental

All experimental details including synthesis, NMR spectra, X-ray crystallography, and theoretical studies can be found in the ESI.†

Data availability

The data supporting this article have been included as part of the ESI.† Crystallographic data for **Ar₃Sb**, **Ar₂SbCl**, **ArSbCl₂** and complexes **1–4** have been deposited at the CCDC under 2313659, 2313660, 2313661, 2313662, 2313664, 2313665, and 2313666.†

Conflicts of interest

There are no conflicts to declare.

Acknowledgements

L. D. and A. R. acknowledge the Czech Science Foundation (project no. 21-02964S). The support from the National Research, Development and Innovation Found for project



K-147095 (for Z.B.) and the EKÖP-24-3-BME-358 project (for Cs.F.) is gratefully acknowledged. We also thank the generous computational resources offered by the Ministry of Education, Youth and Sports of the Czech Republic through the e-INFRA CZ (project: OPEN-31-21).

Notes and references

- 1 For relevant reviews see: (a) V. K. Greenacre, W. Levason and G. Reid, *Coord. Chem. Rev.*, 2021, **432**, 213698; (b) S. L. Benjamin and G. Reid, *Coord. Chem. Rev.*, 2015, **297–298**, 168; (c) W. Levason and G. Reid, *Coord. Chem. Rev.*, 2006, **250**, 2565; (d) N. R. Champnes and W. Levason, *Coord. Chem. Rev.*, 1994, **133**, 115.
- 2 (a) P. Schwab, N. Mahr, J. Wolf and H. Werner, *Angew. Chem., Int. Ed. Engl.*, 1994, **33**, 97; (b) U. Herber, B. Weberndörfer and H. Werner, *Angew. Chem., Int. Ed.*, 1999, **38**, 1609; (c) P. Schwab, J. Wolf, N. Mahr, P. Steinert, U. Herber and H. Werner, *Chem. – Eur. J.*, 2000, **6**, 4471; (d) T. Pechmann, C. D. Brandt and H. Werner, *Dalton Trans.*, 2003, 1495; (e) M. Pietsch, F. P. Gabbaï and M. Scheer, *Z. Anorg. Allg. Chem.*, 2021, **647**, 266.
- 3 M. L. H. A. Green, *J. Organomet. Chem.*, 1995, **500**, 127.
- 4 (a) K. W. Muir and J. A. Ibers, *Inorg. Chem.*, 1969, **8**, 1921; (b) J. M. Burlitch, M. E. Leonowicz, R. B. Petersen and R. E. Hughes, *Inorg. Chem.*, 1979, **18**, 1097.
- 5 (a) A. Amgoune and D. Bourissou, *Chem. Commun.*, 2011, **47**, 859; (b) G. Bouhadir, A. Amgoune and D. Bourissou, *Adv. Organomet. Chem.*, 2010, **58**, 1; (c) G. Bouhadir and D. Bourissou, *Chem. Soc. Rev.*, 2016, **45**, 1065.
- 6 For several examples see: (a) C. A. Miller, T. S. Janik, M. R. Churchill and J. D. Atwood, *Inorg. Chem.*, 1996, **35**, 3683; (b) M. Albrecht, R. A. Gossage, M. Lutz, A. L. Spek and G. van Koten, *Chem. – Eur. J.*, 2000, **6**, 1431; (c) H. Braunschweig, K. Gruss and K. Radacki, *Angew. Chem., Int. Ed.*, 2007, **46**, 7782; (d) H. Braunschweig, K. Gruss and K. Radacki, *Inorg. Chem.*, 2008, **47**, 8595; (e) B. R. Barnett, C. E. Moore, R. Chandrasekaran, S. Sproules, A. L. Rheingold, S. DeBeer and J. S. Figueroa, *Chem. Sci.*, 2015, **6**, 7169; (f) M. Cokoja, C. Gemel, T. Steinke, F. Schroder and R. A. Fischer, *Dalton Trans.*, 2005, 44.
- 7 For several examples see: (a) A. F. Hill, G. R. Owen, A. J. P. White and D. J. Williams, *Angew. Chem., Int. Ed.*, 1999, **38**, 2759; (b) M. J. Lopez-Gomez, N. G. Connelly, M. F. Haddow, A. Hamilton and A. G. Orpen, *Dalton Trans.*, 2010, **39**, 5221; (c) K. Pang, J. M. Tanski and G. Parkin, *Chem. Commun.*, 2008, 1008; (d) S. Senda, Y. Ohki, H. Yasuhiro, T. Tomoko, D. Toda, J. L. Chen, T. Matsumoto, H. Kawaguchi and K. Tatsumi, *Inorg. Chem.*, 2006, **45**, 9914; (e) S. Bontemps, H. Gornitzka, G. Bouhadir, K. Miqueu and D. Bourissou, *Angew. Chem., Int. Ed.*, 2006, **45**, 1611; (f) M. Sircoglou, S. Bontemps, M. Mercy, N. Saffon, M. Takahashi, G. Bouhadir, L. Maron and D. Bourissou, *Angew. Chem., Int. Ed.*, 2007, **46**, 8583; (g) M. Sircoglou, S. Bontemps, G. Bouhadir, N. Saffon, K. Miqueu, W. Gu, M. Mercy, C. H. Chen, B. M. Foxman, L. Maron, O. V. Ozerov and D. Bourissou, *J. Am. Chem. Soc.*, 2008, **130**, 16729; (h) M. Sircoglou, M. Mercy, N. Saffon, Y. Coppel, G. Bouhadir, L. Maron and D. Bourissou, *Angew. Chem., Int. Ed.*, 2009, **48**, 3454; (i) P. A. Rudd, S. Liu, L. Gagliardi, V. G. Young, Jr. and C. C. Lu, *J. Am. Chem. Soc.*, 2011, **133**, 20724; (j) R. C. Cammarota and C. C. Lu, *J. Am. Chem. Soc.*, 2015, **137**, 12486.
- 8 For examples see: (a) J. Grobe, N. Krummen, R. Wehmschulte, B. Krebs and M. Laege, *Z. Anorg. Allg. Chem.*, 1994, **620**, 1645; (b) J. Wagler and E. Brendler, *Angew. Chem., Int. Ed.*, 2010, **49**, 624; (c) P. Gualco, T. P. Lin, M. Sircoglou, M. Mercy, S. Ladeira, G. Bouhadir, L. M. Perez, A. Amgoune, L. Maron, F. P. Gabbaï and D. Bourissou, *Angew. Chem., Int. Ed.*, 2009, **48**, 9892; (d) P. Gualco, M. Mercy, S. Ladeira, L. Maron, A. Amgoune and D. Bourissou, *Chem. – Eur. J.*, 2010, **16**, 10808; (e) M. Karimi, E. S. Tabei, R. Fayad, M. R. Saber, E. O. Danilov, C. Jones, F. N. Castellano and F. P. Gabbaï, *Angew. Chem., Int. Ed.*, 2021, **60**, 22352; (f) M. Karimi and F. P. Gabbaï, *Organometallics*, 2022, **41**, 642; (g) T. P. Lin and F. P. Gabbaï, *Polyhedron*, 2017, **125**, 18; (h) H. Kameo, K. Ikeda, S. Sakaki, S. Takemoto, H. Nakazawa and H. Matsuzaka, *Dalton Trans.*, 2016, **45**, 7570; (i) T. P. Lin and F. P. Gabbaï, *J. Am. Chem. Soc.*, 2012, **134**, 12230; N. Ansmann, J. Munch, M. Schorpp and L. Greb, *Angew. Chem., Int. Ed.*, 2023, **62**, e202313636.
- 9 For reviews see: (a) J. S. Jones and F. P. Gabbaï, *Acc. Chem. Res.*, 2013, **8**, 1720; (b) D. You and F. P. Gabbaï, *Trends Chem.*, 2019, **1**, 485.
- 10 C. R. Wad and F. P. Gabbaï, *Angew. Chem., Int. Ed.*, 2011, **50**, 7369.
- 11 (a) I. S. Ke and F. P. Gabbaï, *Inorg. Chem.*, 2013, **52**, 7145; (b) H. Yan and F. P. Gabbaï, *J. Am. Chem. Soc.*, 2015, **137**, 13425; (c) S. Sen, I. S. Ke and F. P. Gabbaï, *Inorg. Chem.*, 2016, **55**, 9162; (d) J. S. Jones and F. P. Gabbaï, *Chem. – Eur. J.*, 2017, **23**, 1136; (e) S. Sen, I. S. Ke and F. P. Gabbaï, *Organometallics*, 2017, **36**, 4224; (f) Y. H. Lo and F. P. Gabbaï, *Angew. Chem., Int. Ed.*, 2019, **58**, 10194.
- 12 (a) J. S. Jones, C. R. Wade and F. P. Gabbaï, *Angew. Chem., Int. Ed.*, 2014, **53**, 8876; (b) J. S. Jones, C. R. Wade, M. Yang and F. P. Gabbaï, *Dalton Trans.*, 2017, **46**, 5598.
- 13 I. S. Ke and F. P. Gabbaï, *Aust. J. Chem.*, 2013, **66**, 1281.
- 14 (a) C. R. Wade, I. S. Ke and F. P. Gabbaï, *Angew. Chem., Int. Ed.*, 2012, **51**, 478; (b) S. Sahu and F. P. Gabbaï, *J. Am. Chem. Soc.*, 2017, **139**, 5035.
- 15 (a) I. S. Ke, J. S. Jones and F. P. Gabbaï, *Angew. Chem., Int. Ed.*, 2014, **53**, 2633; (b) I. H. Yang and F. P. Gabbaï, *J. Am. Chem. Soc.*, 2014, **136**, 10866; (c) J. S. Jones, C. R. Wade and F. P. Gabbaï, *Organometallics*, 2015, **34**, 2647; (d) D. You and F. P. Gabbaï, *J. Am. Chem. Soc.*, 2017, **139**, 6843; (e) D. You, H. Yang, S. Sen and F. P. Gabbaï, *J. Am. Chem. Soc.*, 2018, **140**, 9644; (f) D. You, J. E. Smith, S. Sen and F. P. Gabbaï, *Organometallics*, 2020, **39**, 4169; (g) R. R. Rodriguez and F. P. Gabbaï, *Molecules*, 2021, **26**,



1985; (h) J. E. Smith, H. Yang and F. P. Gabbaï, *Organometallics*, 2021, **23**, 3886; (i) S. Furan, E. Hupf, J. Boidol, J. Brünig, E. Lork, S. Mebs and J. Beckmann, *Dalton Trans.*, 2019, **48**, 4504.

16 M. Sharma, R. M. Fritz, J. O. Adebajo, Z. Lu, T. R. Cundari, M. A. Omary, A. Choudhury and P. Stavropoulos, *Organometallics*, 2024, **43**, 634.

17 C. Manankandayalage, D. K. Unmruh and C. Krempner, *Chem. – Eur. J.*, 2021, **27**, 6263.

18 P. Pykkö and M. Atsumi, *Chem. – Eur. J.*, 2009, **15**, 186.

19 D. Sharma, A. Benny, R. Gupta, E. D. Jemmins and A. Venugopal, *Chem. Commun.*, 2022, **58**, 11009.

20 L. M. Opris, A. Silvestru, C. Silvestru, H. J. Breunig and E. Lork, *Dalton Trans.*, 2003, 4367.

21 L. Dostál, R. Jambor, A. Růžička and P. Šimon, *Eur. J. Inorg. Chem.*, 2011, 2380.

22 D. Copolovici, F. Isaia, H. J. Breunig, C. I. Rat and C. Silvestru, *RSC Adv.*, 2014, **4**, 26569.

23 T. Řezníček, L. Dostál, A. Růžička, J. Vinklárek, M. Řezáčová and R. Jambor, *Appl. Organomet. Chem.*, 2012, **26**, 237.

24 P. Sharma, D. Castillo, N. Rosas, A. Cabrera, E. Gomez, A. Toscano, F. Lara, S. Hernández and G. Espinosa, *J. Organomet. Chem.*, 2004, **689**, 2593.

25 D. Pérez, P. Sharma, N. Rosas, A. Cabrera, J. L. Arias, F. del Rio-Portilla, J. Vazquez, R. Gutierrez and A. Toscano, *J. Organomet. Chem.*, 2008, **693**, 3357.

26 C. R. Wade, B. L. Murphy, S. Bedajna and F. P. Gabbaï, *Organometallics*, 2024, **43**, 1785–1788.

27 C. K. Webber, F. Kong, J. Kumawat, J. Joy, E. K. Richardson, P. Siano, D. A. Dickie, D. H. Ess and T. B. Gunnoe, *Organometallics*, 2024, **43**, 1789–1802.

